The buoyant cell density of *Cryptococcus neoformans* is affected by capsule size

Raghav Vij, Radames J.B. Cordero, and Arturo Casadevall

Department of Molecular Microbiology and Immunology, Johns Hopkins Bloomberg School of Public Health, 615 North Wolfe Street, Baltimore, MD 21205, USA

Correspondence to: acasade1@jhu.edu

Keywords: cell buoyant density, polysaccharide capsule, melanin, capsular antibody, yeast density, density gradient

ABSTRACT

Cryptococcus neoformans is an environmental pathogenic fungus with a worldwide geographical distribution that is responsible for hundreds of thousands human cryptococcosis cases each year. During infection, the yeast undergoes a morphological transformation involving capsular enlargement that increases microbial volume. To understand the factors that play a role in environmental dispersal of *C. neoformans* and *C. gatii* we evaluated the buoyant cell density of *Cryptococcus* using Percoll isopycnic gradients. We found differences in the buoyant cell density of strains belonging to *C. neoformans* and *C. gatti* species complexes. The buoyant cell density of *C. neoformans* strains varied depending on growth medium conditions. In minimal medium, the cryptococcal capsule made a major contribution to the buoyant cell density such that cells with larger capsules had lower density than those with smaller capsules. Removing the capsule, both by chemical or mechanical methods, decreased the *C. neoformans* cell density. Melanization of the

C. neoformans cell wall, which also contributes to virulence, produced a small but consistent increase in cell density. *C. neoformans* sedimented much slower in seawater as its density approached the density of water. Our results suggest a new function for the capsule whereby it can function as a flotation device to facilitate transport and dispersion in aqueous fluids.

IMPORTANCE

The buoyant cell density of a microbial cell is an important physical characteristic that may affect its transportability in fluids and interactions with tissues during infection. The polysaccharide capsule surrounding *C. neoformans* is required for infection and dissemination in the host. Our results indicate that the capsule has a significant effect on reducing cryptococcal cell density altering its sedimentation in seawater. Modulation of microbial cell density via encapsulation may facilitate dispersal for other important encapsulated pathogens.

INTRODUCTION

C. neoformans and *gattii* species complexes are important fungal pathogens that can cause pulmonary and serious meningeal disease in humans (1). In the environment, *C. neoformans* is commonly found in soil associated with pigeon excreta, while *C. gattii* is most commonly found on trees (2, 3). *C. gattii* have been isolated from marine and fresh water environments (4, 5). Cryptococcal infection occurs via the respiratory tract where yeast particulates can colonize the lungs (6, 7). In immunocompromised patients, *C. neoformans* can readily disseminate from the lungs to other parts of the body, including the central nervous system by crossing the blood brain barrier. The dissemination of *C. neoformans* yeast cells from the lung to the brain is critical in the development of meningeal disease. The yeast cells undergo drastic morphological changes-during this transition that aid its distribution and evasion from host immune mechanisms. For instance, yeast dimensions can range from 1 to 100 μm in diameter by increasing their cell body and/or growing a thick polysaccharide capsule at the cell wall surface in response to immediate environmental conditions (6–9)(8–11).

The polysaccharide capsule is mostly composed of water (12). It is formed by a porous matrix of branched heteropolysaccharides, mainly glucuronoxylomannan, that extends radially from the cell wall (13). Capsule synthesis is induced under certain stressful conditions, and provides protection against host defense mechanisms by acting as a physical barrier, interfering with phagocytosis and sequestering Reactive Oxygen Species (ROS) and drugs (14, 15). The capsule is essential for the virulence of *C. neoformans* and if of interest for both therapeutic and diagnostic strategies (16).

Melanin is another important virulence factor, such that strains that lack the ability to melanize are less pathogenic (16). Melanin is formed by the polymerization of aromatic and/or

phenolic compounds including L-DOPA, methyl-DOPA, epinephrine or norepinephrine (17). In the presence of catecholamine precursors found in the human brain, *Cryptococcus* melanizes its inner cell wall (18). Melanized *C. neoformans* cells are found in the environment (19) and during mammalian infection (20), suggesting an important role of the pigment in *C. neoformans* biology and pathogenesis. Melanization protects cells against a variety of host immune mechanisms and antifungal drugs, as well as, against radiation, desiccation, ROS, and temperature stress (21, 22).

Both the polysaccharide capsule and melanin are complex structures difficult to study. Consequently, it is important to apply biophysical methodologies to gain new insights into the physicochemical properties and biological functions of these major virulence factors (23). One such property that has not been studied in cryptococcal biology is cellular density, presumably a highly-regulated characteristic that may reflect the physiological state of the cell under different conditions (24).

In the first century B.C., Roman writer Vitruvius describes a "Eureka" moment that the Greek polymath Archimedes had when, allegedly, he observed the displacement of water as he sat in a bathtub, which led him to establish the law of buoyancy (25, 26). In a biological context, Archimedes' law (law of buoyancy) can be applied to calculate the ratio of the absolute mass and volume of an organism which could determine whether it floats or sinks in a fluid of given density. During centrifugation in a continuous Percoll density gradient, cells equilibrate upon reaching the point at which the gradient's density matches their own. This allows us to estimate buoyant density of *C. neoformans* and *C. gattii* against bead standards of fixed density.

Buoyant density is used for the separation of cell populations but the factors regulating buoyant cell density in microbiology remain understudied, despite the important role it may play in the migration and dissemination of microbial and mammalian cells in fluids. This could be

because the buoyant cell density depends on many biological and physical factors, which are often difficult to disentangle. Earlier studies found that the buoyant cell density was affected by the osmolality of the medium in which the cells are grown (27, 28), the encapsulation of bacteria by polysaccharide capsule (29) and the stage of cell cycle (30). Strains of *Porphyromonas gingivalis* with lower buoyant density were less susceptible to phagocytosis, however this could be the result of the correlation between buoyant density and cell surface hydrophobicity (31). Other studies have also reported a difference in buoyant density amongst different strains of mycobacteria and *Burkholderia* spp. (32, 33). In the context of eukaryotes, *Saccharomyces cerevisiae* buoyant cell density varies at different stages of cell cycle (34), and quiescent *S. cerevisiae* cell populations can be separated out using density gradients in a stationary phase culture of the yeast (35).

The buoyant cell density (also referred to as cell density) of *C. neoformans* and the factors that affect it have not been previously investigated. In this study, we use Percoll isopycnic gradients to study the effect of capsule induction, antibody treatment, and melanization on the buoyant cell density of *C. neoformans*.

RESULTS

Comparison of *C. neoformans* and *C. gattii* buoyant cell densities

Cell density varied consistently amongst different serotypes of *C. neoformans* and *C. gattii* species complex strains (**Figures 1A&B**). The buoyant density of replicates showed significant variability when comparing *C. neoformans* serotype A (strain H99) to serotype D (strain ATCC 24067) and serotype AD (strain 92.903). However, the density of *C. gatti* did not significantly vary in comparison to *C. neoformans*. To ascertain whether there was a relationship between the density and cell dimension, we imaged the cells with an India-ink counterstain and calculated both the

106 capsule and cell body radii for *C. neoformans* and *C. gatii*. We observed, a statistically significant
107 difference in the cell body radii of all strains when compared to *C. neoformans* serotype A (strain
108 H99). We also observed that the capsule radii of *C. neoformans* Serotype D and AD, and *C. gattii*
109 VG IIa was significantly different when compared to Serotype A.
110
111
112 **Effect of capsule induction on *C. neoformans* buoyant cell density**
113 In vitro, the capsule is induced in stress conditions such as nutrient starvation medium (36).
114 Cells grown in minimal medium (MM) had significantly lower density (**Figure 2A-C**) in
115 comparison to cells grown in nutrient rich conditions (Sabouraud dextrose broth) where the capsule
116 was significantly smaller. The acapsular strains *cap59* had a significantly higher density than
117 encapsulated cells with the same genetic background. Furthermore, we observed no significant
118 differences in the density of acapsular mutants grown in minimal versus rich medium, confirming
119 the contribution of the polysaccharide capsule in determining the cell density in response to
120 different nutrient conditions.
121 Previous studies have reported the molecular composition of the *C. neoformans* capsule by
122 removing the polysaccharide from the cell surface by DMSO extraction and gamma irradiation
123 induced capsule shedding (37). To confirm the effects of the capsule on the buoyant cell density,
124 encapsulated H99 cells were treated with gamma radiation and DMSO to remove capsular material
125 (**Figure 3**). We observed a significant increase in cell density when the capsule was removed by
126 both treatments indicating that the polysaccharide capsule influences the cell density.
127
128 **Capsule size correlates with buoyant cell density**

129 Linear regression analysis revealed that capsule radii correlates with cell uch that yeast with larger
130 capsules were less dense (**Figure 4A)**. There was no significant relationship between cell body
131 size and cell density (**Figure 4B**).
132
133 **Encapsulated *Cryptococcus neoformans* settles slower in sea water**
134 We tested whether the low density of encapsulated *C. neoformans* allowed the fungi to
135 float in water or seawater. The density of seawater is 1.0236 g/ cc at room temperature (38, 39),
136 and density of *C. neoformans* in minimal medium is 1.022 +/- 0.008165. When *C. neoformans*
137 grown in minimal medium was added to a cuvette containing seawater, a large population of cells
138 became suspended in the seawater, which became turbid (**Figure 5A**). This effect was not seen
139 with PBS where the cells sink to the bottom within 3 hours (**Figure 5B**).
140
141 **Melanization increases *C. neoformans* buoyant cell density**
142 Comparison of melanized and non-melanized H99 *C. neoformans* cells demonstrated that
143 melanization was associated with a moderate increase in cell density (**Figure 6)**. Since the increase
144 in the density was small, and melanized cell can easily be distinguished visually from non-
145 melanized cell, we mixed the melanized and non-melanized cells in 1:1 ratio before loading the
146 samples onto the density gradient. While non-melanized cells displayed a range of density that
147 overlapped with melanized cells, the latter tended to have higher density when compared to non-
148 melanized cells inoculated from the same sabouraud broth pre-culture. Isolated melanin
149 'ghosts'(40) had much greater density than cells, estimated to be > 1.1 g/ cc (data not shown). Note
150 that melanized cells also had smaller capsules (**Figure 6D, ii**), which may contribute to the increase
151 in cell density. Thus, we also compared the density of melanized and non-melanized cells after

152 removal of the capsule by gamma radiation (**Figure 6C, ii**). Upon capsule removal, we observed
153 that the density of melanized cells was consistently and significantly higher than non-melanized
154 cells.
155
156 **Antibody binding and other conditions that have no significant effect on *C. neoformans***
157 **buoyant cell density**
158 Previous studies have shown that capsular antibodies alter the viscoelastic properties and structure
159 of the capsule (41). Antibody binding also causes a change in the hydration state of the PS capsule
160 (12). Treatment of H99 *C. neoformans* with capsular antibodies (18B7 and E1) did not
161 significantly alter the cell buoyant density (Figure **S1**). Furthermore, binding of mouse
162 complement, incubations at different salt concentration (to induce osmotic stress) and incubation
163 in lipid rich medium had no significant impact on *C. neoformans* buoyant cell density (Figure **S2**).
164
165 **DISCUSSION**
166 In this study, we characterized the buoyant cell density of *C. neoformans* and *C. gattii* in
167 different conditions. We report minor differences in buoyant densities between serotypes of the
168 cryptococcal species complex. Our results also suggest that the capsule plays a major role in
169 determining the buoyant cell density of the yeast such that encapsulated strains have densities close
170 to that of water. Meanwhile, melanization increased the density slightly. Changes in buoyancy
171 could influence the dispersal of the yeast in the environment, and dissemination of the fungal
172 pathogen during infection. Furthermore, the buoyant density may be used for the separation of
173 different populations of yeast cells (35), to characterize *C. neoformans* mutants with capsular
174 defects (16) and for the isolation of the titan cells (42).

175 The buoyant density of a microbe is a fundamental biophysical property that influences its
176 behavior in aqueous fluids. Depending on its density, a microbe could remain suspended in a fluid
177 or settle to the bottom. Amongst other factors, this could influence the microbe's access to
178 nutrients, sunlight and oxygen. Thus, it is not surprising that marine and freshwater unicellular
179 organisms including phytoplankton, regulate their cell density via mechanisms that involve the
180 synthesis and storage of gas vacuoles, polysaccharide mucilage sheaths, and glycogen (43).
181 Interestingly, the polysaccharide mucilage sheath of these bacteria, that resembles the
182 polysaccharide capsule of *C. neoformans*, has been characterized as an important factor that
183 decreases the density of the cell to just below the density of water (44). Our data demonstrates that
184 the cryptococcal capsule serves a similar function by increasing the volume of the yeast cell
185 without significantly increasing its mass and thereby reducing its density.
186 A quantitative parameter used to determine how fast a population of microbial cells sinks
187 in a fluid of given density is the settling velocity, which is calculated by the Stoke's law and
188 depends on the buoyant density and the size (diameter) for a spherical object such as a yeast cell
189 (43, 45). In marine bacteria, low cell density (< 1.064 g/cc) correlates with low settling velocity
190 as calculated by Stoke's law (46). The variable size of *C. neoformans* grown in minimal medium
191 (3-16 μm) and the low density (~ 1.022 g/cc) we observed during nutrient starvation conditions in
192 an aqueous environment suggests that the settling velocity of *C. neoformans* would be similarly
193 low. More importantly, the encapsulated *C. neoformans* cells would have a lower settling velocity
194 when compared to similar-sized cells that have no capsule due to the decrease in density.
195 We hypothesize that the capsule can function as a flotation device that allows the yeast cell
196 to flow horizontally in aqueous environment to access (47) nutrients, oxygen and disperse the
197 pathogen (48). For instance, a study found that a *C. gattii* clinical isolate survived in filtered ocean

198 water, distilled water and saline water (up-to 10% of initial inoculum) at room temperature up to
199 94 days (49). The resistance of *Cryptococcus* to different levels of osmotic stress is consistent with
200 our observations that high salt concentrations do not alter the cell density. The strains of *C.*
201 *neoformans* and *C. gattii* have heterogeneous global distribution, and the mechanism of the
202 dispersal are unknown (50). Possibly; the varied density of the strains influences the differential
203 dispersal of the fungal pathogen. Thus, in the context of environmental fungal pathogens *C.*
204 *neoformans* and *gattii*, the cell density could play an important role in determining the dispersal
205 of the yeast in the environment and affect its ability to infect a wide range of hosts, including
206 marine mammals such as dolphins (51–53). Estimating the settling velocity of microbial cells in
207 aqueous fluids will add weight to the hypothesis that the buoyant density of *C. neoformans* and *C.*
208 *gattii* influences environmental dispersal.

209 Melanization had a moderate influence on cell density. Despite the much greater density
210 of melanin ghosts, cellular melanization had a small effect on cell density presumably due to the
211 fact that melanin contributes approximately only 15.4% (m/m) of cellular mass (40).

212 In immunocompromised hosts, the *C. neoformans* can disseminate from the lungs to the
213 brain where it causes life-threatening meningitis. This multistep process could require the fungal
214 cell to travel into the draining lymph node and into fluidic blood and lymph systems to survive and
215 grow outside the lungs. Murine models have shown that the capsule and cell body size is different
216 at different sites of infection (9). Our results showing that the capsule makes an important
217 contribution to reducing buoyant density and increasing flotation suggests that the capsular
218 enlargement that occurs during infection could be a major variable in determining dissemination
219 in body fluids.

In summary, the density of *C. neoformans* grown in minimal medium is slightly greater than that of water. The presence of a capsule reduced the density such that it approached that of water. Hence, the capsule, by reducing density, also reduces the settling velocity of *C. neoformans* in aqueous solutions, which could favor environmental dispersal. The establishment of *C. gattii* in the Pacific Northwest is reported to have occurred relatively recently (50). Although the means by which *C. gattii* reached North America are unknown the fact that it has been recovered from marine environments (49) together with our finding of a low density of yeast cells indicating a propensity of the pathogen to float suggest that sea currents could have transported *C. gattii* between continents. The observation that the polysaccharide capsule makes a large contribution to reducing density suggests a new role for this structure in the environment as an aid to cell dispersal and transport in aqueous fluids.

ACKNOWLEDGEMENT

AC was supported by grants 5R01HL059842, 5R01AI033774, 5R37AI033142, and 5R01AI052733. We would like to thank Dr. Francoise Dromer (Institut Pasteur) for providing capsular antibody ES1 (IgG). R.V. designed and conducted the experiments, analyzed the data and wrote the manuscript. R.J.B.C. and A.C. contributed to the experimental design, supervised the experiments, edited and wrote parts of the manuscript.

239 **MATERIALS AND METHODS**

240

241 **Yeast cultures**

242 Frozen stocks of *C. neoformans* and *gatti* strains were inoculated into Sabouraud agar rich medium
243 (pH adjusted to 7.4) at 30°C for 48 hours. Yeast cultures of *C. neoformans* included

Species	Strain	Reference or Source
C. neoformans	H99	John Perfect (Durham, NC)
	Cap59	(54)
C. neoformans	ATCC24067	ATCC (Manassas, VA)
C. neoformans hybrids	MAS92-203	(55)
C. gatii	NIH444, ATCC32609	(55)
	106.93	(55)
	VGI, WM179	ATCC (Manassas, VA)
	VGIIa, R265	ATCC (Manassas, VA)

244 Acapsular mutants from *Cryptococcus neoformans* cultured included Cap59 (Background H99,
245 serotype A). Approximately 10^6 cells from the stationary phase cultures in Sabouraud broth were
246 washed twice in Minimal Medium (10 mM $MgSO_4$, 29.3 mM KH_2PO_4, 13 mM glycine, 3 µM
247 thiamine-HCl, and 15 mM dextrose with pH adjusted to 5.5). The washed cells were inoculated
248 into Minimal Medium (MM) for capsule induction, MM with L-DOPA (100 mM) to induce
249 melanization, and Sabouraud broth for providing rich medium conditions. Cells were incubated at
250 37°C for 48 hours, rotating at 180 RPM. Cells were washed twice with sterile PBS (Phosphate
251 Buffer Saline), centrifuging them for 5 minutes at 4700 x *g*. Cells were counted using a
252 hemocytometer, and dilutions were made to obtain 1 X 10^7 cells in PBS. The cells were then loaded

253 onto Percoll Density gradients with or without treatments to test the effect of different conditions
254 on the buoyant cell density.
255

256 **Density gradient centrifugation**

257 Percoll is a non-toxic and isotonic alternative to the commonly used sucrose gradient, and is
258 composed of polyvinylpyrrolidone coated colloidal silica particles (56). Percoll has found
259 applications for separation of mammalian blood, tumor, immune and endothelial cells, and
260 microbial cells due to its ability to form reproducible self-generated continuous gradients (57).
261 Stock Isotonic Percoll (SIP) was obtained by added 1 part of 1.5 M NaCl to 9 parts of Percoll. The
262 working solution of 70% (v/v) was obtained by diluting SIP with 0.15 M NaCl, to a final density
263 of 1.0914 g/ml. Three milliliters of this solution were loaded into polycarbonate ultracentrifuge
264 tubes (13 X 51 mm). Approximately, 10^7 cells were pelleted at 4700 x *g* and over layered directly
265 or after treatment. All gradients were run in parallel with a standard tube.
266 For the preparation of the standard tube, 10 µl of each uniform density bead standard (Cospheric
267 DMB kit) including light orange (ORGPMS-1.00 250-300um, density 1.00 g/cc), fluorescent
268 green (1.02 g/cc), florescent orange (1.04 g/cc), florescent violet (1.06 g/cc), dark blue (1.08) and
269 florescent red (1.099 g/cc), was loaded and mixed with the Percoll.
270 By varying time and speed of centrifugation, it was found that the most optimal separation of the
271 density gradient beads, which was taken as an indication for the most optimal continuous density
272 gradient formed, occurred at 40,000 RPM for 30 minutes (acceleration 9, deceleration 0), in TLA
273 100.3 fixed angle rotor in Optima TLX tabletop ultracentrifuge.
274

Buoyant cell density estimation

First, the images of the density gradient were taken under uniform light and shadow conditions using Nikon D3000 DSLR, Auto settings. Next, pixel area measurements were taken from the bottom of the tube, to the area at the beginning of each band (a1), ranging to the end of each band (a2), to the upper meniscus of the tube (f). The density factor, $D_f(min, max)$, and the average along with the standard deviation was computed on Microsoft Xcel according to the following formulae,

$$D_f(min, max) = \left\{\left(\frac{f - a_1}{f}\right), \left(\frac{f - a_2}{f}\right)\right\}$$

A standard curve was derived, where D_f (min, max) and buoyant density (g/l) of the density marker beads were computed by linear regression. A 95% confidence interval was used to interpolate the mean density of sample cells, around a standard deviation, run in parallel with the uniform density bead standards.

Although, the results from different Percoll gradient runs follow the same trend, the exact density values can vary considerably. This can be attributed to pipetting errors or errors in measurement of density factor.

Gamma irradiation of cells for capsule removal

Gamma irradiation was used to remove the capsule as described earlier (58). Approximately 10^9 cells of melanized and non-melanized cells were plated on a 24-well plate. The cells were irradiated to a total dose of 1500 Gy, using Shepherd Mark 1 at the SKCCC Experimental Irradiator Core at Johns Hopkins University Sidney Kimmel Comprehensive Cancer Center. Cells were washed twice in PBS and approximately 10^7 cells were pelleted at 4700 x *g* and loaded onto the gradient.

297

298 **DMSO Extraction of *C. neoformans* capsule**

299 Approximately 10^7 cells were incubated in 15 ml of DMSO at 30°C for 30 minutes to allow capsule
300 extraction. The cells were washed thrice in 1X PBS, pelleted and loaded onto the Percoll density
301 gradient.

302

303 **Antibody Coating of *C. neoformans* capsule**

304 Purified antibodies, 18B7 and E1 (kindly provided by the Dromer's laboratory), were obtained
305 from stock solutions kept at 4°C. The antibodies were serially diluted in PBS to concentrations of
306 20µg, 10µg, 1 µgand 0.1 µg/ml. A pellet of 10^7 cells was suspended with 1 ml of each Ab solution
307 in Eppendorf tubes, vortexed and incubated at 28°C on a rotating mixer, for 1 hour.

308

309 ***C. neoformans* melanization**

310 Frozen stalks of *C. neoformans* H99 was inoculated into Sabouraud broth and incubated at 30°C
311 for 48 hours, till the cultures reached stationary phase. The cells were counted using a
312 hemocytometer. 10^6 cells/ml of were inoculated into minimal medium (10 mM MgSO4, 29.3
313 mM KH2PO4, 13 mM glycine, 3 µM thiamine-HCl, and 15 mM dextrose with pH adjusted to 5.5)
314 with and without L-DOPA (100 mM). The cells were cultured for 10 days at 30°C rotating at 180
315 RPM. The cells were washed twice in PBS, and 10^7 cells were pelleted at 47000 x *g* loaded of
316 melanized, non-melanized and 1:1 mixture of the cells was loaded onto the gradient. Melanin
317 ghosts were prepared as described (40).

318

319 **Mouse complement deposition in *C. neoformans***

320 Frozen stocks of guinea pig complement (1 mg/ml) were thawed. 50% (500 g/ml), 20%, 10% and
321 1% dilutions with PBS was added a pellet of 10^7 cells. The cells were incubated with complement
322 for 1 hour at 28°C in a rotating-mixer.

323

324 **Providing *C. neoformans* with osmotic stress**

325 *C. neoformans* (approximately 10^8 cells) were incubated with 1 ml of 10X PBS, 1X PBS, 0.1X
326 PBS and ultrapure distilled water (MilliQ) for 2 hours in 30 rotating-mixer at 28°C.

327

328 **Settling of *C. neoformans* in seawater**

329 10^7 cells of C. neoformans grown in MM were gently pipetted onto cuvettes containing 3ml of sea
330 water (Worldwide Imports AWW84130 Live Nutri Seawater) and PBS. The settling of the cells
331 was observed by imaging the cuvettes at different time intervals with a Nikon D3000 DSLR. The
332 images were analyzed using image J. The relative displacement was measured using the following
333 formulae (f-u)/f, where f is the area of the tube, u is the area from the bottom of the tube to the
334 upper menisci of cells that are settling.

335

336 **Cell imaging and yeast size measurements**

337 The cells were visualized and imaged with India Ink negative staining under Olympus AX70
338 Microscope at 20X magnification and 40X magnification. The capsule and cell body size was
339 estimated using an automated measurement Python software (59) or by ImageJ when cells were
340 observed to be aggregated.

341

342 **Statistical analysis**

343 All statistical analysis was performed on GraphPad Prism 7.0 software. The density of cells was
344 estimated by using making a standard curve from beads of different densities using linear
345 regression to estimate the unknown values of a given sample with a 95% confidence interval.
346 Details of statistical tests applied are provided on the figure legends.

347

REFERENCE

1. Perfect JR. 2000. Cryptococcosis, p. 79–93. *In* Atlas of Infectious Diseases. Current Medicine Group, London.

2. Ellis DH, Pfeiffer TJ. 1990. Natural habitat of Cryptococcus neoformans var. gattii. J Clin Microbiol 28:1642–1644.

3. Emmons CW. 1960. Prevalence of Cryptococcus neoformans in pigeon habitats. Public Health Rep 75:362–364.

4. Bartlett KH, Kidd SE, Kronstad JW. 2008. The emergence of Cryptococcus gattii in British Columbia and the Pacific Northwest. Curr Infect Dis Rep 10:58–65.

5. MacDougall L, Kidd SE, Galanis E, Mak S, Leslie MJ, Cieslak PR, Kronstad JW, Morshed MG, Bartlett KH. 2007. Spread of Cryptococcus gattii in British Columbia, Canada, and Detection in the Pacific Northwest, USA. Emerg Infect Dis 13:42–50.

6. Neilson JB, Fromtling RA, Bulmer GS. 1977. Cryptococcus neoformans: size range of infectious particles from aerosolized soil. Infect Immun 17:634–638.

7. Powell KE, Dahl BA, Weeks RJ, Tosh FE. 1972. Airborne Cryptococcus neoformans: particles from pigeon excreta compatible with alveolar deposition. J Infect Dis 125:412–415.

8. Feldmesser M, Kress Y, Casadevall A. 2001. Dynamic changes in the morphology of Cryptococcus neoformans during murine pulmonary infection. Microbiology 147:2355–2365.

9. Charlier C, Chrétien F, Baudrimont M, Mordelet E, Lortholary O, Dromer F. 2005. Capsule Structure Changes Associated with Cryptococcus neoformans Crossing of the Blood-Brain Barrier. Am J Pathol 166:421–432.

10. Zaragoza O, García-Rodas R, Nosanchuk JD, Cuenca-Estrella M, Rodríguez-Tudela JL, Casadevall A. 2010. Fungal Cell Gigantism during Mammalian Infection. PLoS Pathog 6.

371 11. Okagaki LH, Strain AK, Nielsen JN, Charlier C, Baltes NJ, Chrétien F, Heitman J,
372 Dromer F, Nielsen K. 2010. Cryptococcal Cell Morphology Affects Host Cell Interactions and
373 Pathogenicity. PLOS Pathog 6:e1000953.
374 12. Maxson ME, Cook E, Casadevall A, Zaragoza O. 2007. The volume and hydration of the
375 Cryptococcus neoformans polysaccharide capsule. Fungal Genet Biol 44:180–186.
376 13. Cordero RJB, Pontes B, Guimarães AJ, Martinez LR, Rivera J, Fries BC, Nimrichter L,
377 Rodrigues ML, Viana NB, Casadevall A. 2011. Chronological Aging Is Associated with
378 Biophysical and Chemical Changes in the Capsule of Cryptococcus neoformans. Infect Immun
379 79:4990–5000.
380 14. Casadevall A, Coelho C, Cordero RJB, Dragotakes Q, Jung E, Vij R, Wear MP. 2018.
381 The Capsule of Cryptococcus neoformans. Virulence 0.
382 15. Zaragoza O, Rodrigues ML, De Jesus M, Frases S, Dadachova E, Casadevall A. 2009.
383 The capsule of the fungal pathogen Cryptococcus neoformans. Adv Appl Microbiol 68:133–216.
384 16. Kwon-Chung KJ, Rhodes JC. 1986. Encapsulation and melanin formation as indicators of
385 virulence in Cryptococcus neoformans. Infect Immun 51:218–223.
386 17. Garcia-Rivera J, Eisenman HC, Nosanchuk JD, Aisen P, Zaragoza O, Moadel T,
387 Dadachova E, Casadevall A. 2005. Comparative analysis of Cryptococcus neoformans acid-
388 resistant particles generated from pigmented cells grown in different laccase substrates. Fungal
389 Genet Biol 42:989–998.
390 18. Nosanchuk JD, Stark RE, Casadevall A. 2015. Fungal Melanin: What do We Know
391 About Structure? Front Microbiol 6.
392 19. Nosanchuk JD, Rudolph J, Rosas AL, Casadevall A. 1999. Evidence That Cryptococcus
393 neoformans Is Melanized in Pigeon Excreta: Implications for Pathogenesis. Infect Immun

394 67:5477–5479.

395 20. Nosanchuk JD, Rosas AL, Lee SC, Casadevall A. 2000. Melanisation of Cryptococcus

396 neoformans in human brain tissue. The Lancet 355:2049–2050.

397 21. Casadevall A, Rosas AL, Nosanchuk JD. 2000. Melanin and virulence in Cryptococcus

398 neoformans. Curr Opin Microbiol 3:354–358.

399 22. Cordero RJB, Casadevall A. 2017. Functions of fungal melanin beyond virulence. Fungal

400 Biol Rev 31:99–112.

401 23. Frases S, Viana NB, Casadevall A. 2011. Biophysical Methods for the Study of

402 Microbial Surfaces. Front Microbiol 2.

403 24. Grover WH, Bryan AK, Diez-Silva M, Suresh S, Higgins JM, Manalis SR. 2011.

404 Measuring single-cell density. Proc Natl Acad Sci 108:10992–10996.

405 25. Biello D, Biello D. 2006. Fact or Fiction?: Archimedes Coined the Term “Eureka!” in the

406 Bath. Sci Am.

407 26. Kuroki H. 2016. How did Archimedes discover the law of buoyancy by experiment?

408 Front Mech Eng 11:26–32.

409 27. Baldwin WW, Myer R, Powell N, Anderson E, Koch AL. 1995. Buoyant density

410 ofEscherichia coli is determined solely by the osmolarity of the culture medium. Arch Microbiol

411 164:155–157.

412 28. Baldwin WW, Kubitschek HE. 1984. Evidence for osmoregulation of cell growth and

413 buoyant density in Escherichia coli. J Bacteriol 159:393–394.

414 29. Lowe BA, Miller JD, Neely MN. 2007. Analysis of the Polysaccharide Capsule of the

415 Systemic Pathogen Streptococcus iniae and Its Implications in Virulence. Infect Immun

416 75:1255–1264.

417 30. Kubitschek HE. 1987. Buoyant density variation during the cell cycle in microorganisms.
418 Crit Rev Microbiol 14:73–97.
419 31. Sundqvist G, Figdor D, Hänström L, Sörlin S, Sandström G. 1991. Phagocytosis and
420 virulence of different strains of Porphyromonas gingivalis. Eur J Oral Sci 99:117–129.
421 32. Sagripanti J-L, Carrera M, Robertson J, Levy A, Inglis TJJ. 2011. Size distribution and
422 buoyant density of Burkholderia pseudomallei. Arch Microbiol 193:69–75.
423 33. Vijay S, Nair RR, Sharan D, Jakkala K, Mukkayyan N, Swaminath S, Pradhan A, Joshi
424 NV, Ajitkumar P. 2017. Mycobacterial Cultures Contain Cell Size and Density Specific Sub-
425 populations of Cells with Significant Differential Susceptibility to Antibiotics, Oxidative and
426 Nitrite Stress. Front Microbiol 8.
427 34. Baldwin WW, Kubitschek HE. 1984. Buoyant density variation during the cell cycle of
428 Saccharomyces cerevisiae. J Bacteriol 158:701–704.
429 35. Allen C, Büttner S, Aragon AD, Thomas JA, Meirelles O, Jaetao JE, Benn D, Ruby SW,
430 Veenhuis M, Madeo F, Werner-Washburne M. 2006. Isolation of quiescent and nonquiescent
431 cells from yeast stationary-phase cultures. J Cell Biol 174:89–100.
432 36. Zaragoza O, Casadevall A. 2004. Experimental modulation of capsule size in
433 Cryptococcus neoformans. Biol Proced Online 6:10–15.
434 37. Frases S, Nimrichter L, Viana NB, Nakouzi A, Casadevall A. 2008. Cryptococcus
435 neoformans Capsular Polysaccharide and Exopolysaccharide Fractions Manifest Physical,
436 Chemical, and Antigenic Differences. Eukaryot Cell 7:319–327.
437 38. Nayar KG, Sharqawy MH, Banchik LD, Lienhard V JH. 2016. Thermophysical
438 properties of seawater: A review and new correlations that include pressure dependence.
439 Desalination 390:1–24.

440 39. Sharqawy MH, Lienhard JH, Zubair SM. 2010. Thermophysical properties of seawater: a
441 review of existing correlations and data. Desalination Water Treat 16:354–380.
442 40. Wang Y, Aisen P, Casadevall A. 1996. Melanin, melanin "ghosts," and melanin
443 composition in Cryptococcus neoformans. Infect Immun 64:2420–2424.
444 41. Cordero RJB, Pontes B, Frases S, Nakouzi AS, Nimrichter L, Rodrigues ML, Viana NB,
445 Casadevall A. 2013. Antibody Binding to Cryptococcus neoformans Impairs Budding by
446 Altering Capsular Mechanical Properties. J Immunol Author Choice 190:317–323.
447 42. Zaragoza O, Nielsen K. 2013. Titan cells in Cryptococcus neoformans: cells with a giant
448 impact. Curr Opin Microbiol 16:409–413.
449 43. Reynolds CS, Oliver RL, Walsby AE. 1987. Cyanobacterial dominance: The role of
450 buoyancy regulation in dynamic lake environments. N Z J Mar Freshw Res 21:379–390.
451 44. Reynolds CS. 2007. Variability in the provision and function of mucilage in
452 phytoplankton: facultative responses to the environment. Hydrobiologia 578:37–45.
453 45. Richardson TL, Jackson GA. 2007. Small Phytoplankton and Carbon Export from the
454 Surface Ocean. Science 315:838–840.
455 46. Inoue K, Nishimura M, Nayak BB, Kogure K. 2007. Separation of marine bacteria
456 according to buoyant density by use of the density-dependent cell sorting method. Appl Env
457 Microbiol 73:1049–1053.
458 47. Condie SA, Bormans M. 1997. The Influence of Density Stratification on Particle
459 Settling, Dispersion and Population Growth. J Theor Biol 187:65–75.
460 48. Kidd SE, Bach PJ, Hingston AO, Mak S, Chow Y, MacDougall L, Kronstad JW, Bartlett
461 KH. 2007. Cryptococcus gattii Dispersal Mechanisms, British Columbia, Canada. Emerg Infect
462 Dis 13:51–57.

463 49. Kidd SE, Chow Y, Mak S, Bach PJ, Chen H, Hingston AO, Kronstad JW, Bartlett KH.
464 2007. Characterization of Environmental Sources of the Human and Animal Pathogen
465 Cryptococcus gattii in British Columbia, Canada, and the Pacific Northwest of the United States.
466 Appl Environ Microbiol 73:1433–1443.
467 50. Roe CC, Bowers J, Oltean H, DeBess E, Dufresne PJ, McBurney S, Overy DP, Wanke B,
468 Lysen C, Chiller T, Meyer W, Thompson GR, Lockhart SR, Hepp CM, Engelthaler DM. 2018.
469 Dating theCryptococcus gattiiDispersal to the North American Pacific Northwest. mSphere 3.
470 51. Gales N, Wallace G, Dickson J. 1985. Pulmonary cryptococcosis in a striped dolphin
471 (Stenella coeruleoalba). J Wildl Dis 21:443–446.
472 52. Migaki G, Gunnels RD, Casey HW. 1978. Pulmonary cryptococcosis in an Atlantic
473 bottlenosed dolphin (Tursiops truncatus). Lab Anim Sci 28:603–606.
474 53. Miller WG, Padhye AA, van Bonn W, Jensen E, Brandt ME, Ridgway SH. 2002.
475 Cryptococcosis in a Bottlenose Dolphin (Tursiops truncatus) Caused by Cryptococcus
476 neoformans var. gattii. J Clin Microbiol 40:721–724.
477 54. Coelho C, Souza ACO, Derengowski L da S, de Leon-Rodriguez C, Wang B, Leon-
478 Rivera R, Bocca AL, Gonçalves T, Casadevall A. 2015. Macrophage mitochondrial and stress
479 response to ingestion of Cryptococcus neoformans. J Immunol Baltim Md 1950 194:2345–2357.
480 55. Cordero RJB, Frases S, Guimaräes AJ, Rivera J, Casadevall A. 2011. Evidence for
481 branching in cryptococcal capsular polysaccharides and consequences on its biological activity.
482 Mol Microbiol 79:1101–1117.
483 56. Pertoft H, Rubin K, Kjellén L, Laurent TC, Klingeborn B. 1977. The viability of cells
484 grown or centrifuged in a new density gradient medium, Percoll(TM). Exp Cell Res 110:449–
485 457.

486 57. Pertoft H. 2000. Fractionation of cells and subcellular particles with Percoll. J Biochem
487 Biophys Methods 44:1–30.
488 58. Bryan RA, Zaragoza O, Zhang T, Ortiz G, Casadevall A, Dadachova E. 2005.
489 Radiological studies reveal radial differences in the architecture of the polysaccharide capsule of
490 Cryptococcus neoformans. Eukaryot Cell 4:465–475.
491 59. Dragotakes Q, Casadevall A. 2018. Automated Measurement of Cryptococcal Species
492 Polysaccharide Capsule and Cell Body. J Vis Exp JoVE.
493

494 # FIGURES

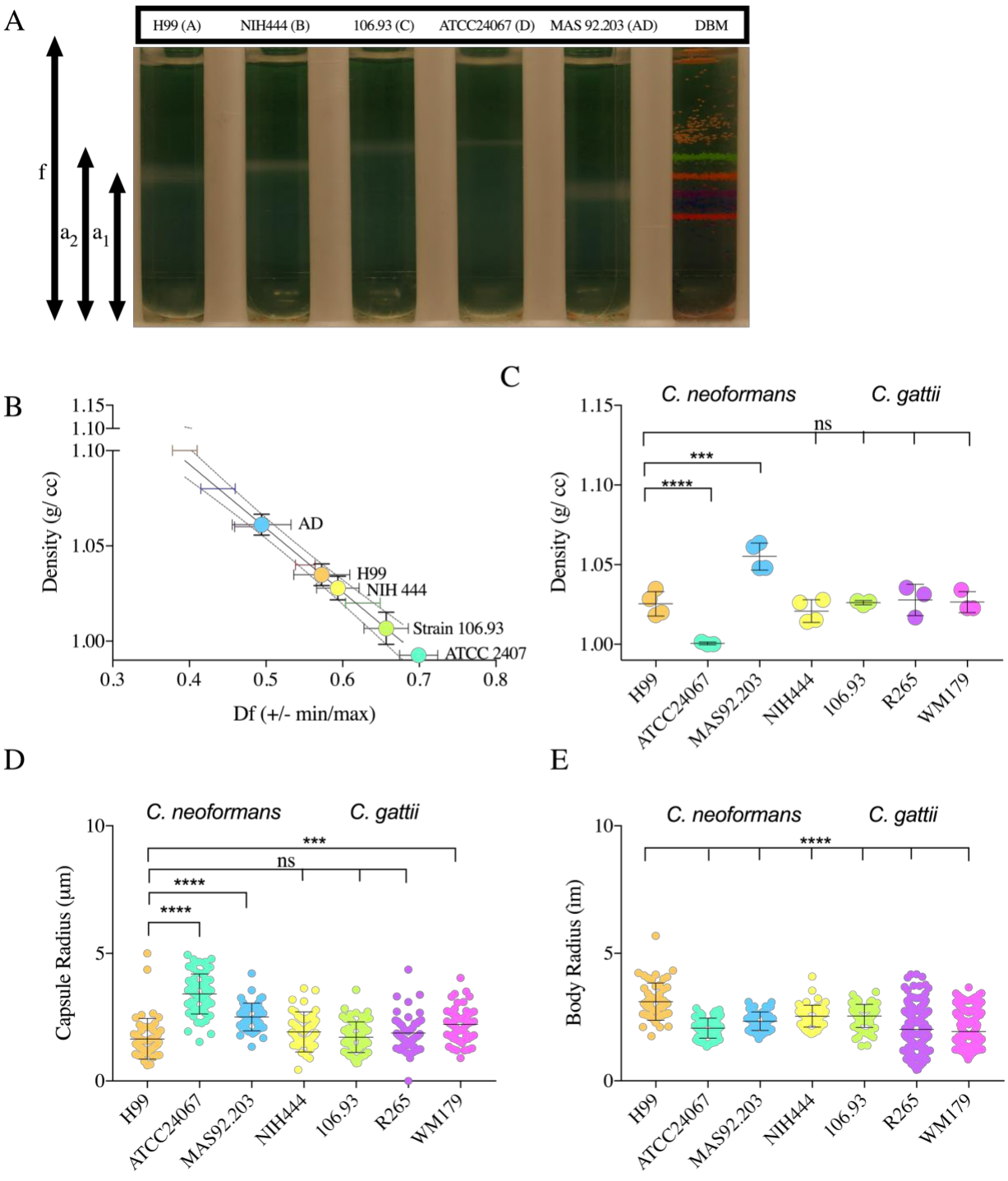

495

496 **Figure 1: The buoyant cell density of *C. neoformans* and *C. gattii* serotypes.**

A. Representative image of 3-4 independent repetitions of Percoll density gradients comparing the buoyant density of *C. neoformans* (Serotype A, D and AD) and *C. gattii* (Serotype B, C) to density bead markers (DBM). **B.** Representative data from 4 independent experiments depicting the line interpolation of the density factor (min, max) calculated by pixel areas as per the formulae ($f - a_1/f$, $f - a_2/f$). The df (min, max) values of the density marker beads are used to estimate the buoyant cell density of the cells ran in parallel. **C.** Histogram depicting the difference in buoyant cell density of different serotypes of *C. neoformans* (Serotype A, AD and D) and *C. gattii* (Serotype B, C and variants VGI, VGIIa). The experiment was performed 3 times, as indicated by the symbols on the bar graph, the error bar represents the SD about the mean. **D.** Representative data of capsule *i.* and cell body *ii.* radii of different serotypes and strains. One-way ANOVA was used to for the comparison of cell density, capsule and cell body radii of different strains and serotypes of *C. neoformans* and *C. gattii* to the respective measurements of H99 strain of *C. neoformans*. The following symbols were used to annotate the statistical significance ns ($P > 0.05$), * ($P \leq 0.05$), ** ($P \leq 0.01$), *** $P \leq 0.001$, **** $P \leq 0.0001$

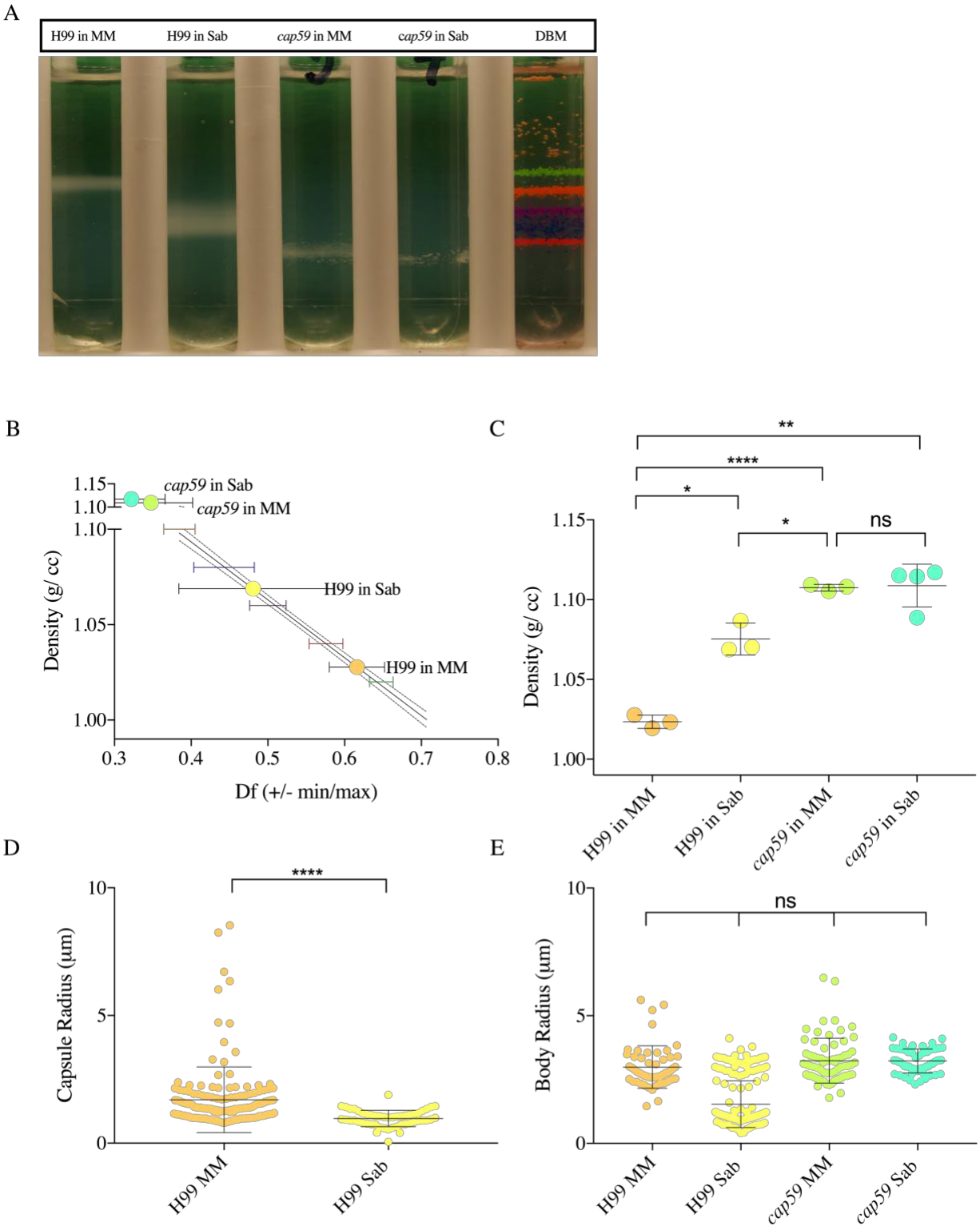

Figure 2: Induction of capsule synthesis decreases *C. neoformans* cell buoyant density.

A. Representative image of three independent repetitions of Percoll density gradients showing the density of *C. neoformans* H99 juxtaposed with acapsular mutant *Cap59*, both grown in sabouraud medium (Sab), minimal medium (MM). **B.** Representative data from three independent experiments depicting a line interpolation of the density factor with the buoyant densities of the bead standards to calculate the buoyant cell densities of the gradients run in parallel. **C.** Histogram depicting a decrease in the range of buoyant cell density in H99 cells grown in MM, when compared to Sab, due to capsule induction. *Cap59* mutant are significantly denser than normal H99 cells grown in MM. Experiments were performed in replicates independently, as indicated by the data points on the histogram, except for *Cap59* in Sab was performed once as indicated by the symbols on the bar graph, error bar represents SD about the mean. **D.** Representative data depicts *i.* the capsule radii and *ii.* the cell body radii of different strains *C. neoformans* H99 grown in different medium conditions (MM, Sab). *Cap59* grown in MM and Sab do not have a capsule, therefore the capsule radii were not quantified. One-way ANOVA was used to for the comparison of cell density, capsule and cell body radii of *C. neoformans* Cap59 and H99 gown in different conditions. The following symbols were used to annotate the statistical significance ns ($P > 0.05$), * $P \leq 0.05$), ** ($P \leq 0.01$), *** $P \leq 0.001$, **** $P \leq 0.0001$ (For the last two choices only)

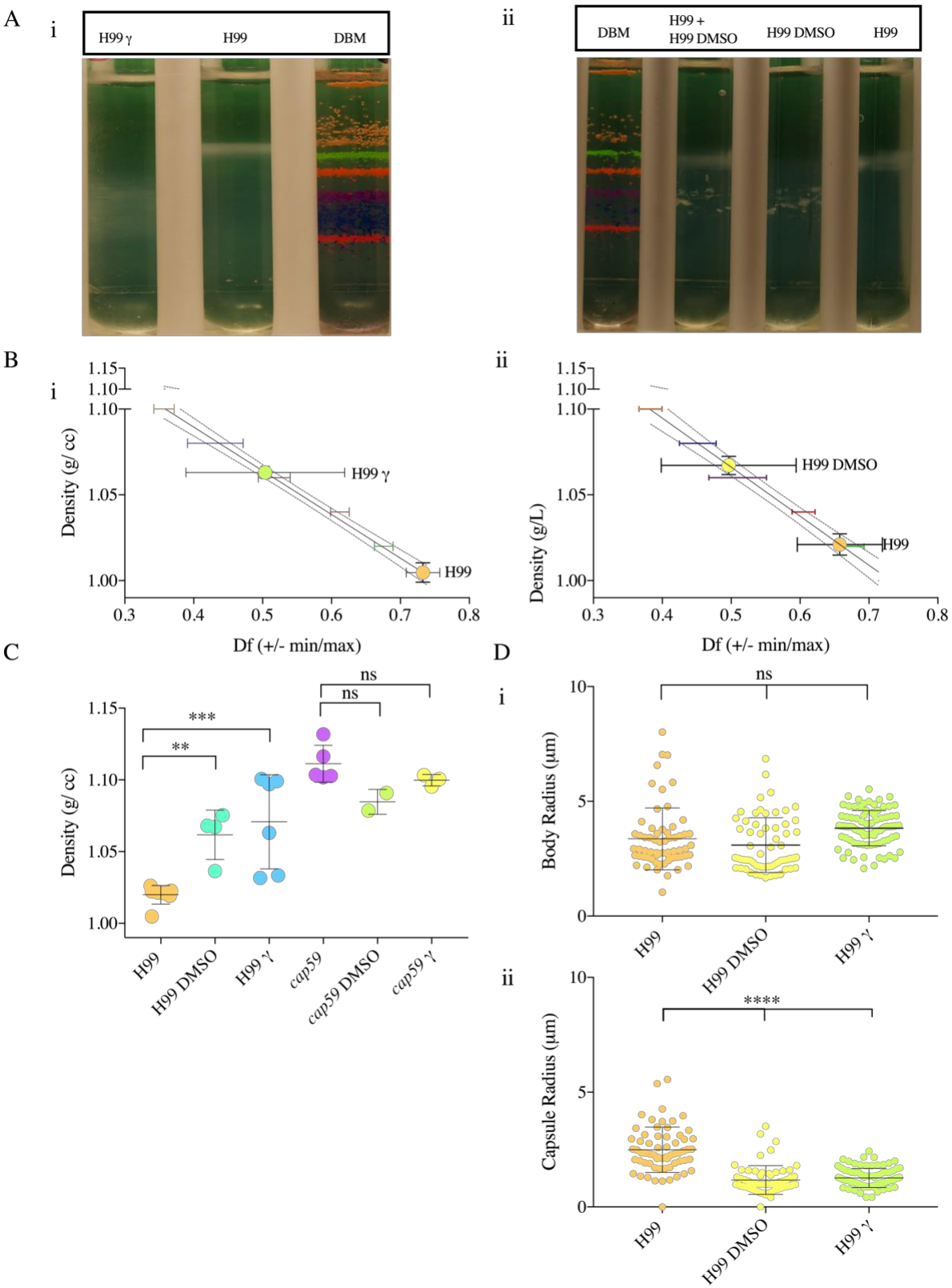

Figure 3: Removal of *C. neoformans* increases the buoyant cell density. **A.** *i* Representative image of four independent repetitions of Percoll density gradients comparing the buoyant cell densities of irradiated (γ) and non-irradiated *C. neoformans* (H99) with a standard of colored uniform density beads. *ii* Representative image of four independent Percoll density gradients of encapsulated *C. neoformans* H99 strains before and after DMSO extraction. **B.** *i, ii* Representative data from independent experiments depicting a line interpolation of the density factor (df) with the buoyant densities of the bead standards, to calculate the buoyant cell densities of *C. neoformans* before and after extraction of the capsule, run in parallel. **C.** A histogram depicting buoyant density of *C. neoformans* before and after capsule extraction by γ rays and DMSO. The irradiation experiment was performed independently thrice, and the capsular extraction by DMSO twice, as indicated by the symbols on the bar graph, error bar represents SD about the mean. One-way ANOVA was used to determine differences in density of H99 and Cap59 treated with DMSO and gamma radiation with H99 and Cap59 grown in MM for 10 ds respectively. **D.** Representative data depicts *i.* the capsule radii and *ii.* the cell body radii of *C. neoformans* before and after gamma irradiation capsule shedding. One-way ANOVA was used to for the comparison of cell density, capsule and cell body radii of different strains and serotypes of *C. neoformans* and *C. gattii* to the respective measurements of H99 strain of *C. neoformans*. The following symbols were used to annotate the statistical significance ns ($P > 0.05$), * ($P \leq 0.05$), ** ($P \leq 0.01$), *** $P \leq 0.001$, **** $P \leq 0.0001$ (For the last two choices only)

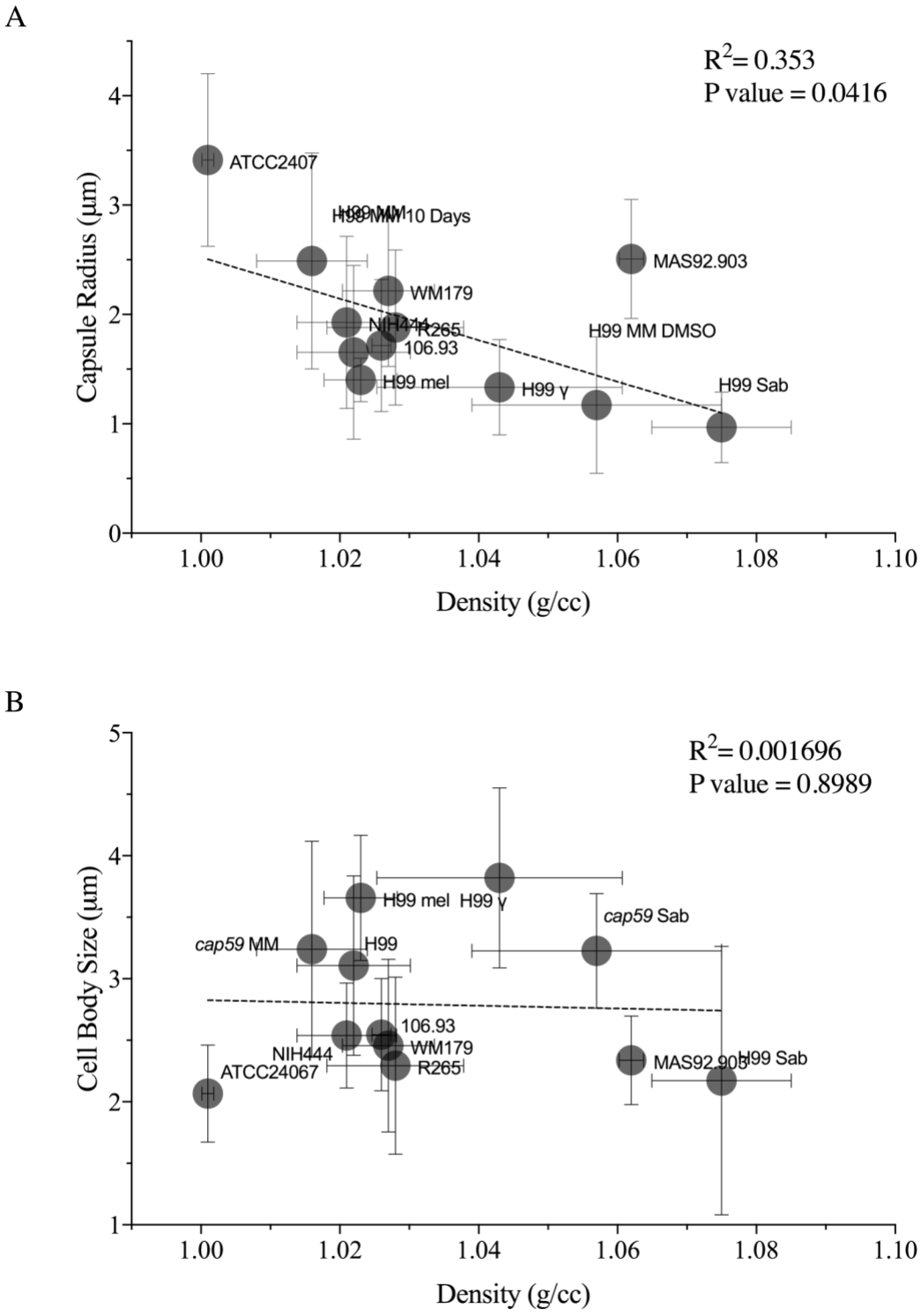

Figure 4: The density of *C. neoformans* and *C. gattii* correlates with the capsule radii A. Density (g/ cc) significantly correlates linearly with the capsule size (µm). **B.** No linear relationship was found in when comparing the cell body size (radii) to the density. The density values were

collated from all the experiments performed for a specific condition (n= 3 to 5). The cell size was taken from a single experiment for each condition which was found to representative of the replicates.

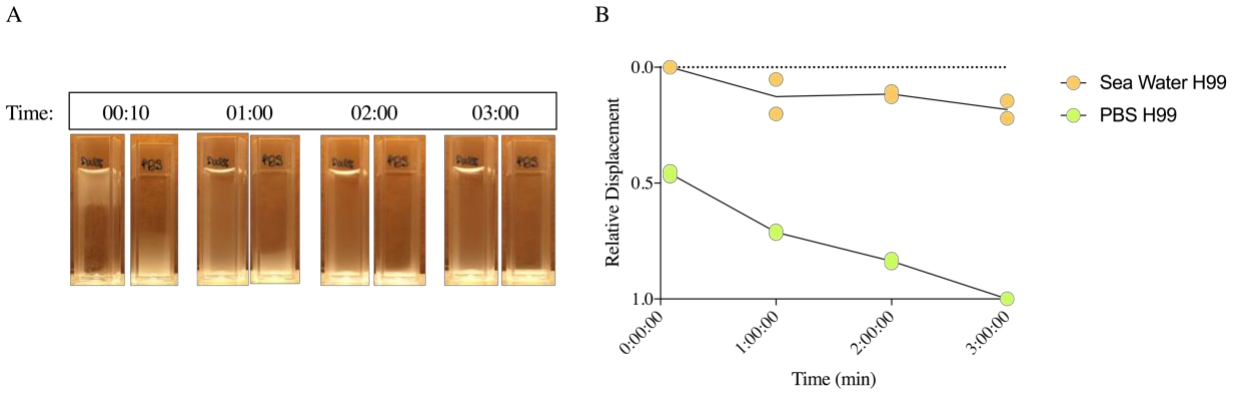

Figure 5: Encapsulated C. neoformans settles slower in seawater A. Representative image of cuvettes (3mL) containing seawater (left) and PBS (right) imaged at different time points shows that H99 grown in MM settles faster in PBS. **B.** Graphical representation of normalized displacement of the upper menisci of cells settling in sea water and PBS. Each data point on a line at a given time-point represents an independent experiment (n=2).

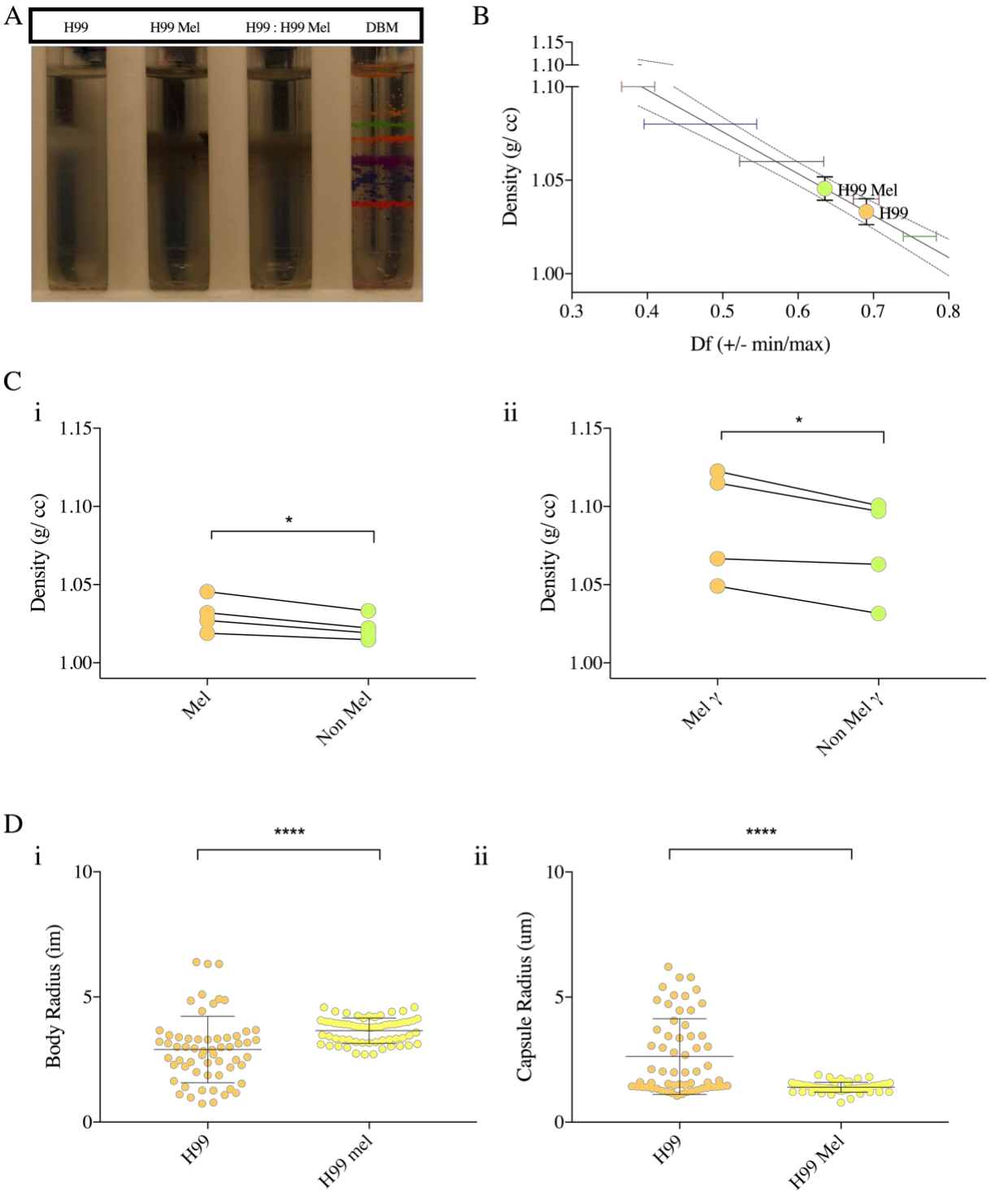

Figure 6: Effect of Melanization on *C. neoformans* buoyant cell density. A. Representative image of four independent repetitions of Percoll density gradients comparing the density of H99 in MM, H99 in MM with L-DOPA (mel) and a 1:1 mixture of the cells. The white cells (H99) band slightly above the melanized black cells (mel) as can be seen by the gradient that contains the mixture. **B.** Representative data from three independent experiments depicting a line

interpolation of the density factor with the buoyant densities of the bead standards, to calculate the buoyant cell densities of the gradients run in parallel. **C.** *i.* A histogram depicting density of mel and non-mel *C. neoformans* to compare the density of a mel and non-mel culture started from the same sabouraud pre-culture. The experiment was performed in replicates (n=4), as indicated by the symbols on the bar graph. A paired t-test found the pairing to be significant (**) and found consistent and significant differences (*) between non melanised and melanised cells. *ii.* A histogram depicting the density of and non-mel cells after removal of capsule by gamma radiation. The experiment was performed in pairs, such that the paired cultures were inoculated from the same sabouraud pre-culture and were treated with gamma-radiation (1500 Gy) together. A paired t-test found the pairing to be significant (*) and found consistent and significant differences (*) between non melanised and melanised cells treated with gamma radiation. **D.** Representative data depicts *i.* the capsule radii and *ii.* the cell body radii of melanized and non-melanized *C. neoformans*. One-way ANOVA was used to for the comparison of capsule and cell body radii of melanised and non-melanised H99 strain of *C. neoformans*. The following symbols were used to annotate the statistical significance ns ($P > 0.05$), * ($P \leq 0.05$), ** ($P \leq 0.01$), *** $P \leq 0.001$, **** $P \leq 0.0001$ (For the last two choices only)

SUPPLEMENTARY FIGURES

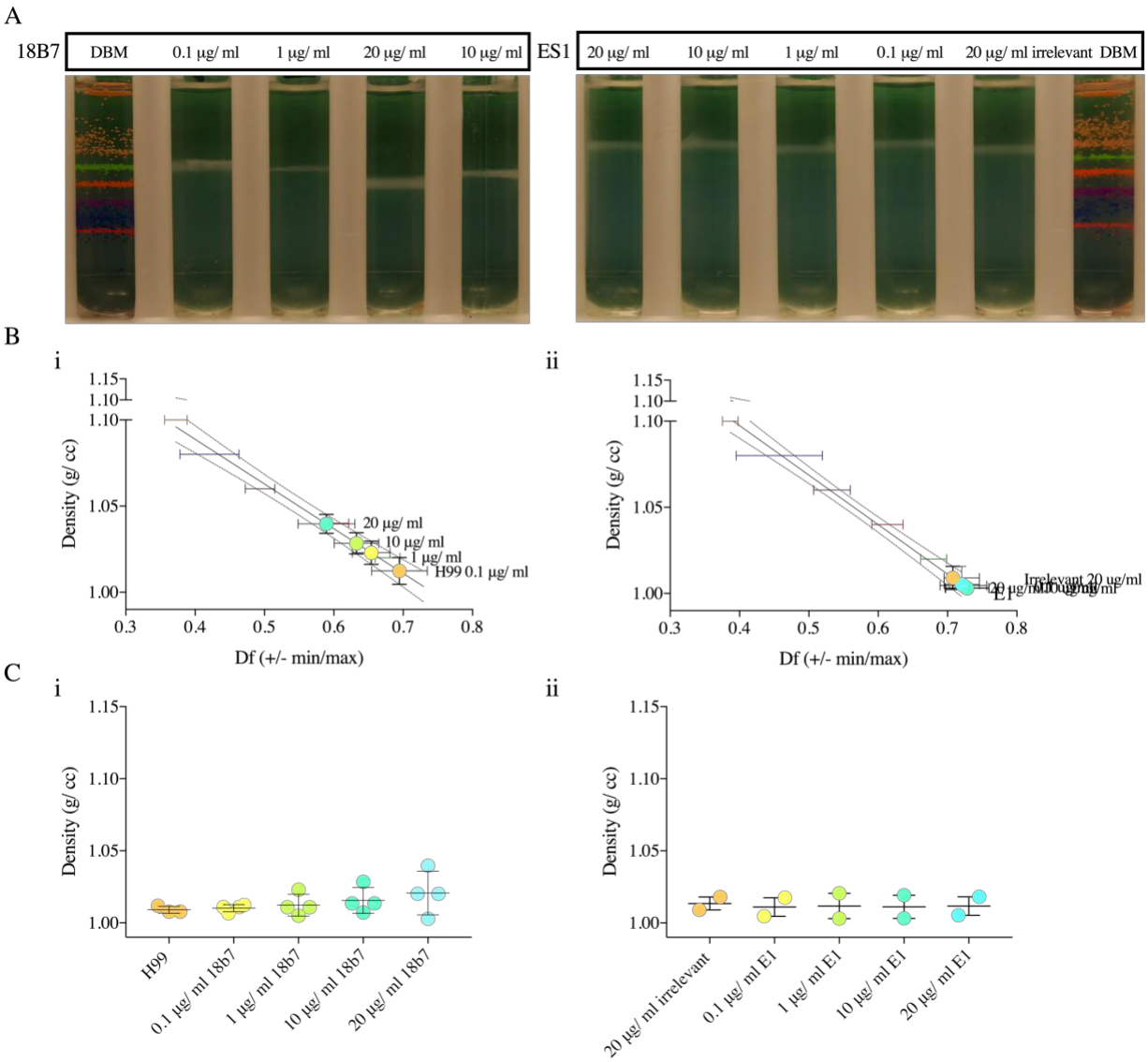

Figure S1: Binding of capsular antibodies do not alter *C. neoformans* buoyant density. **A.** Representative image of independent repetitions of Percoll density gradients comparing the density of *C. neoformans* H99 with and without antibody incubation with i. 18B7 and ii. ES1. **B.** Representative data independent experiments depicting a line interpolation of the density factor with the buoyant densities of the bead standards, to calculate the buoyant cell densities of the gradients run in parallel. **C.** *i.* A histogram depicting density of *C. neoformans* H99 incubated with capsular antibodies i. 18B7 (n=4) and ii. ES1 (n=2) at different concentrations (0.1,1,10,20 µg/ mL)

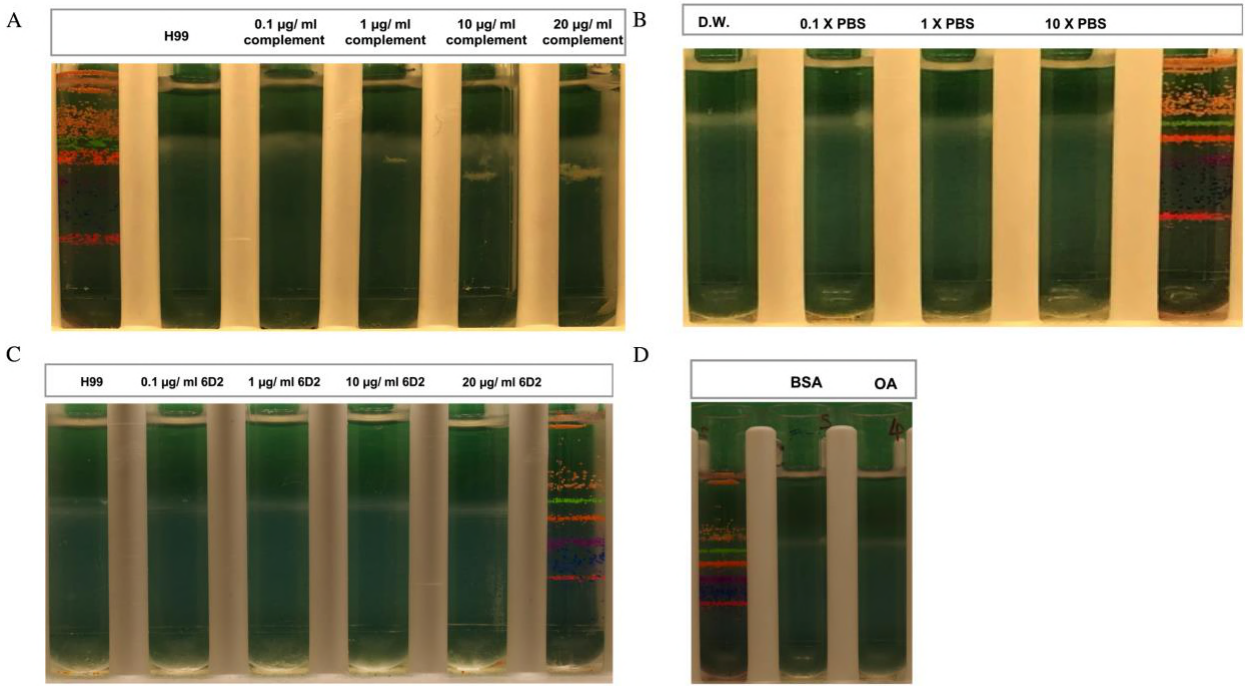

Figure S2 Effect of complement binding, osmotic shock, melanin-binding antibody and growth in rich lipid media on buoyant density. Image of Percoll density gradients comparing the density of *C. neoformans* H99 upon **A.** complement binding, **B.** osmotic shock, **C.** 6D2 antibody binding **D.** growth in lipid rich media. These conditions do not affect the buoyant cell density of *Cryptococcus neoformans* (H99) significantly. Experiments were done once.

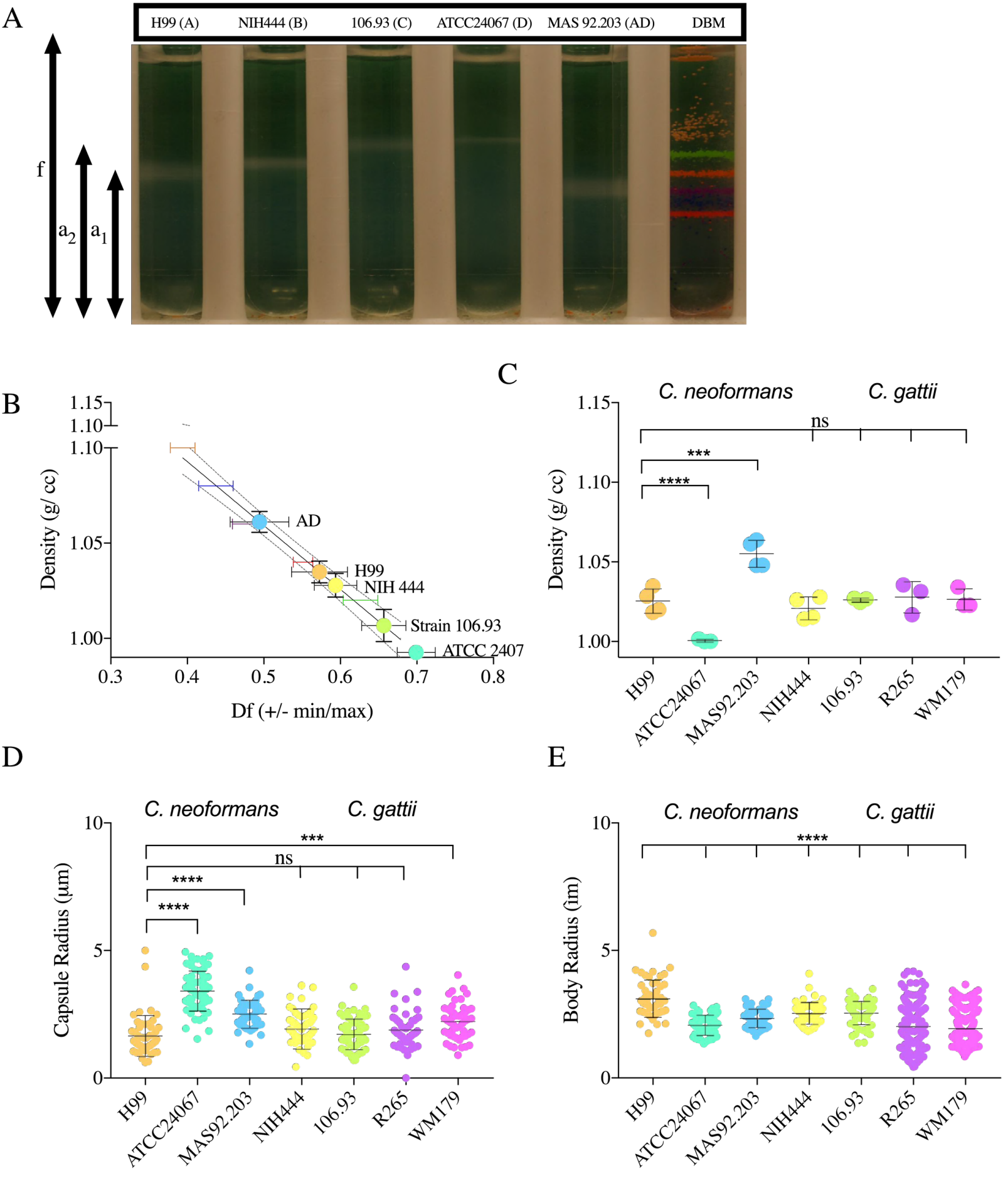
A
H99 (A)
NIH444 (B)
106.93 (C)
ATCC24067 (D)
MAS 92.203 (AD)
DBM
f
a2
a1
B
Density (g/ cc)
Df (+/- min/max)
AD
H99
NIH 444
Strain 106.93
ATCC 2407
C
C. neoformans
C. gattii
ns
***
****
Density (g/ cc)
H99
ATCC24067
MAS92.203
NIH444
106.93
R265
WM179
D
C. neoformans
C. gattii
***
ns
****
****
Capsule Radius (µm)
E
C. neoformans
C. gattii
****
Body Radius (im)

A

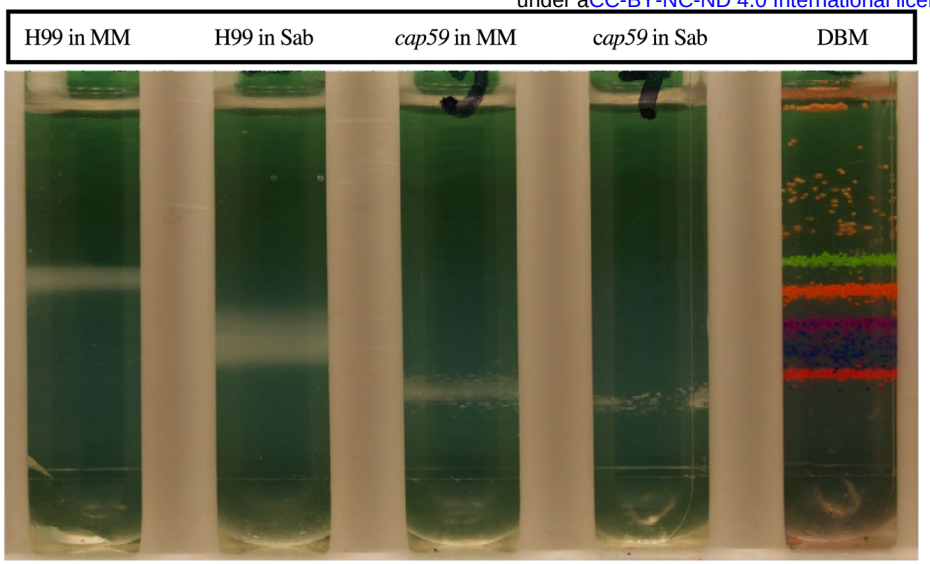

B

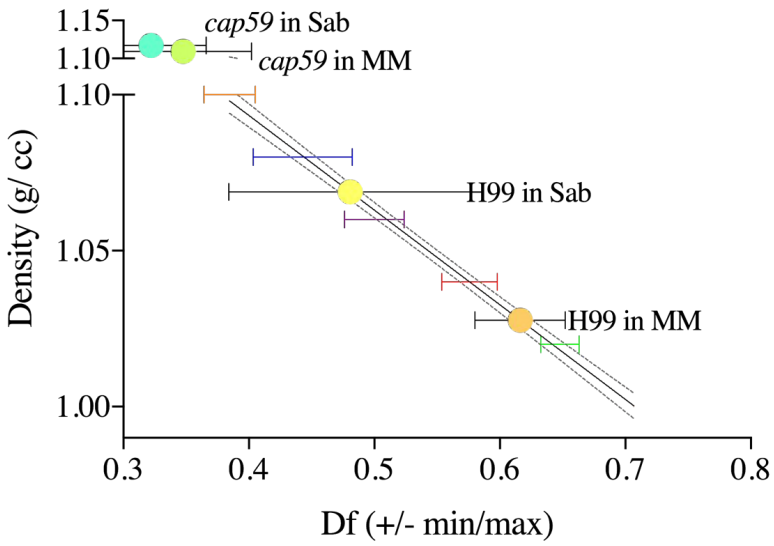

C

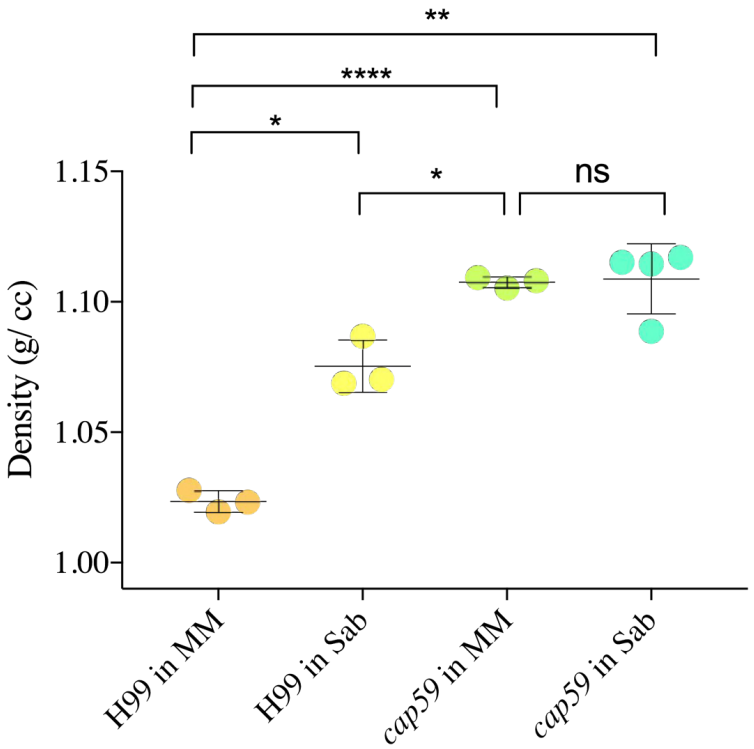

D

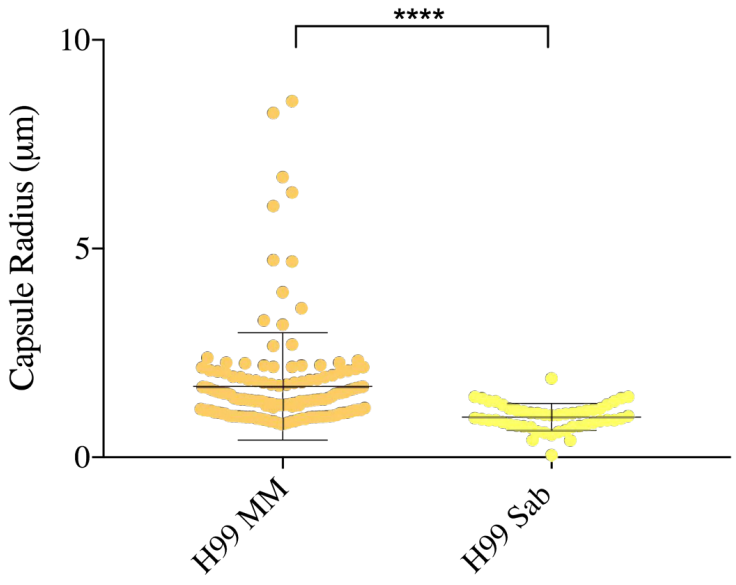

E

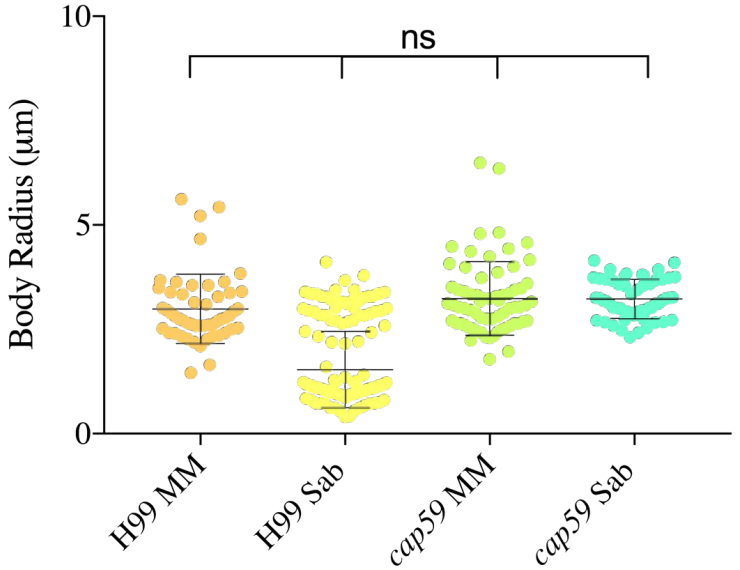

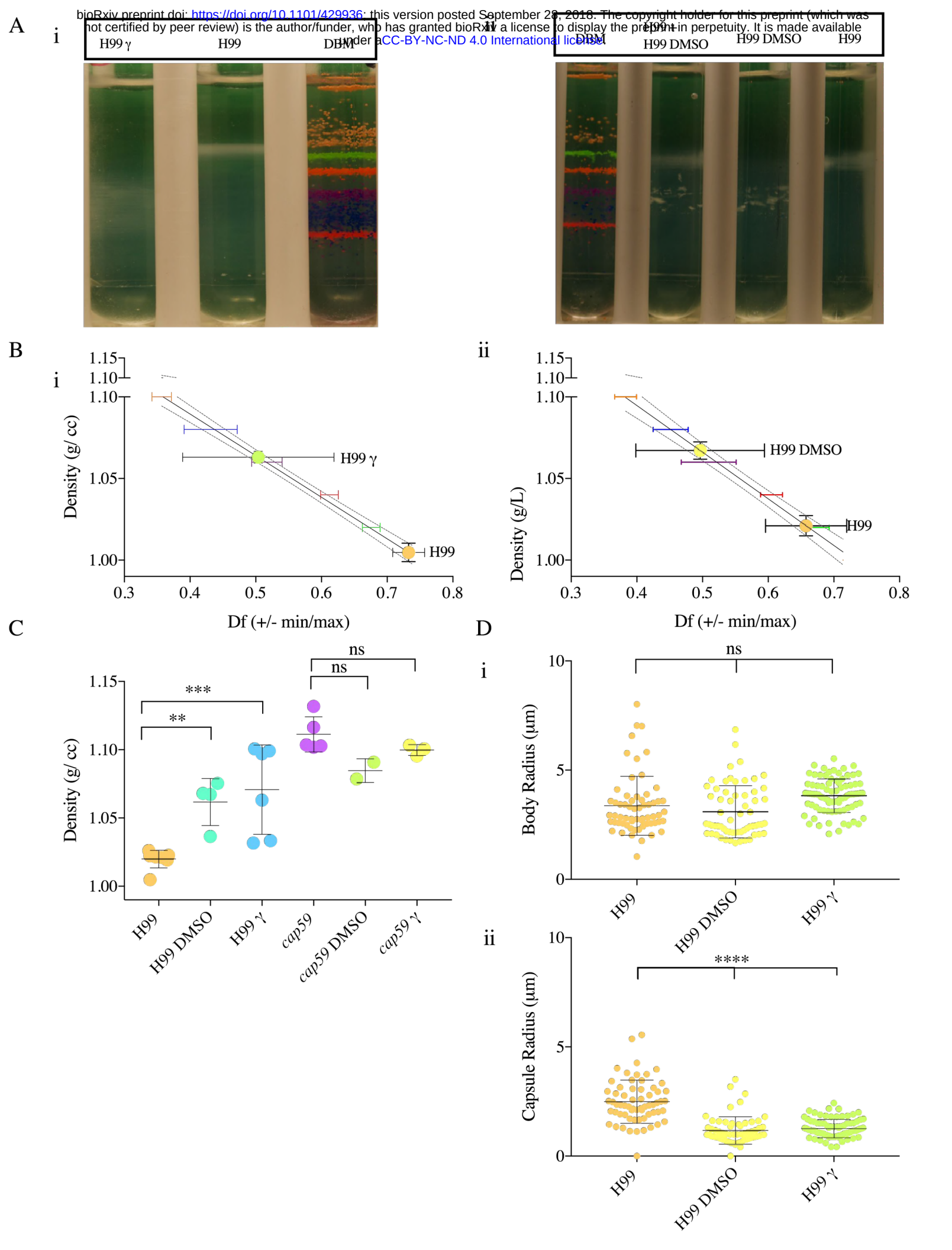

A

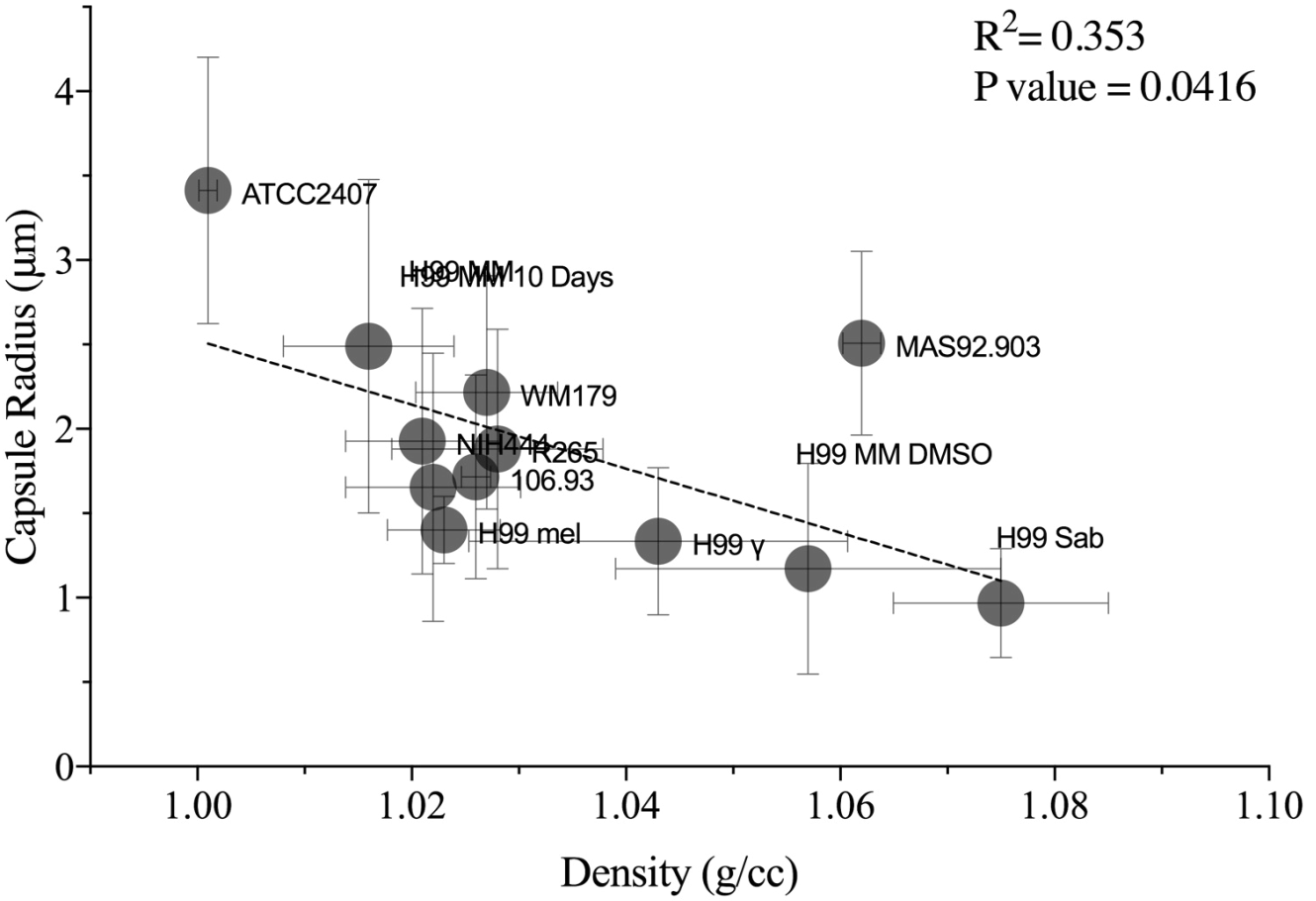

B

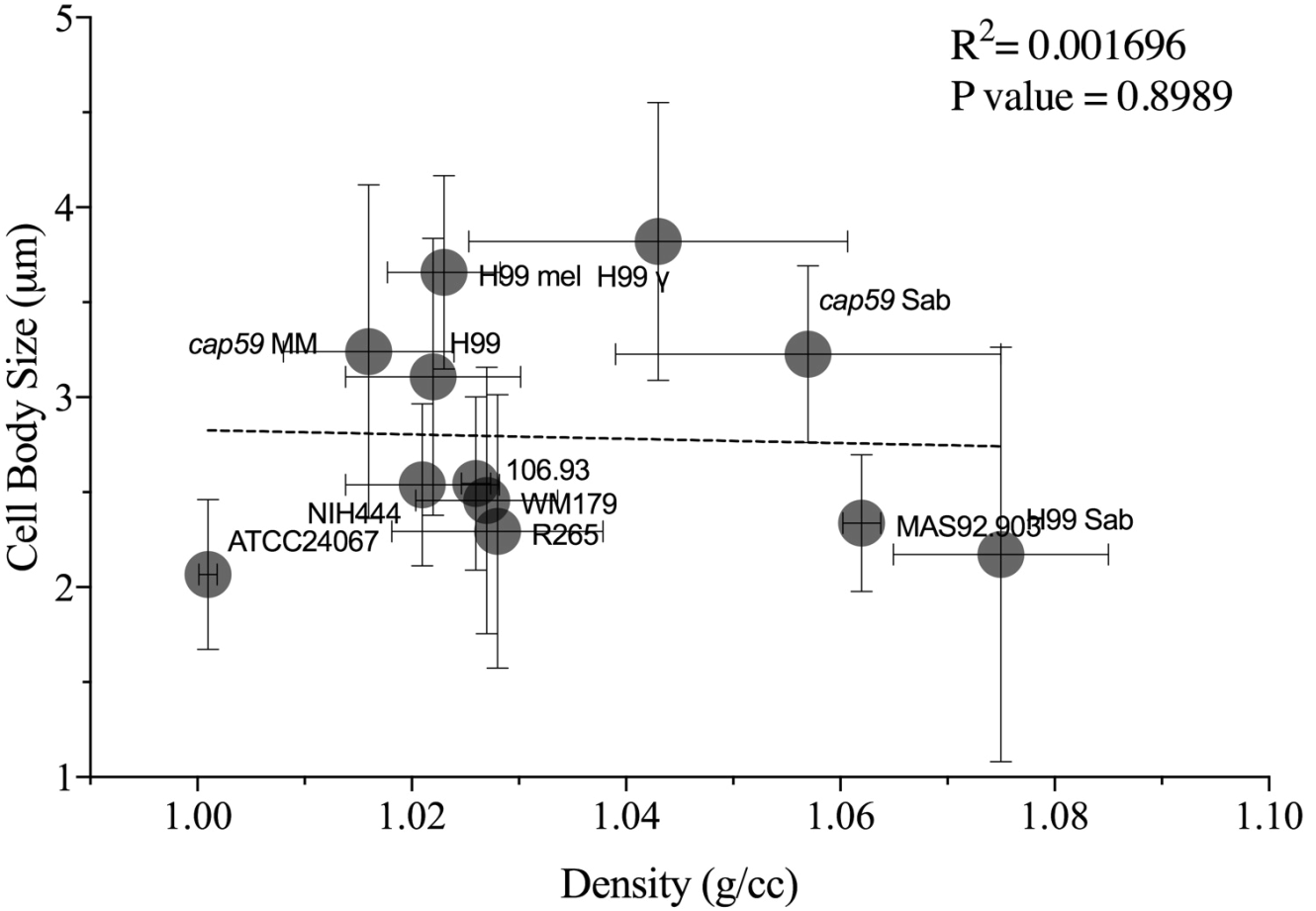

A

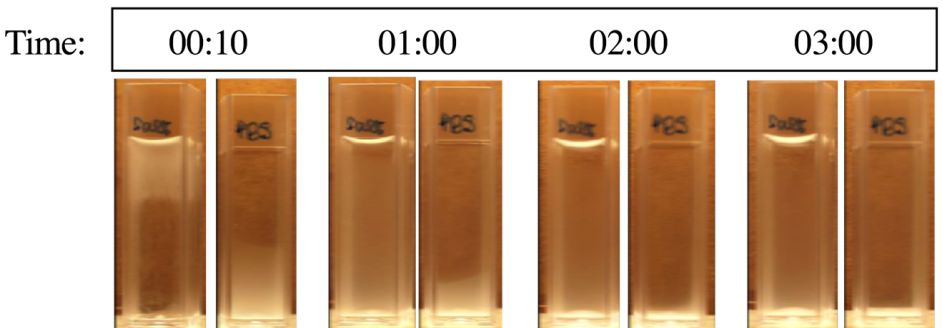
Time:
00:10
01:00
02:00
03:00
PBS
PBS
PBS
PBS

B

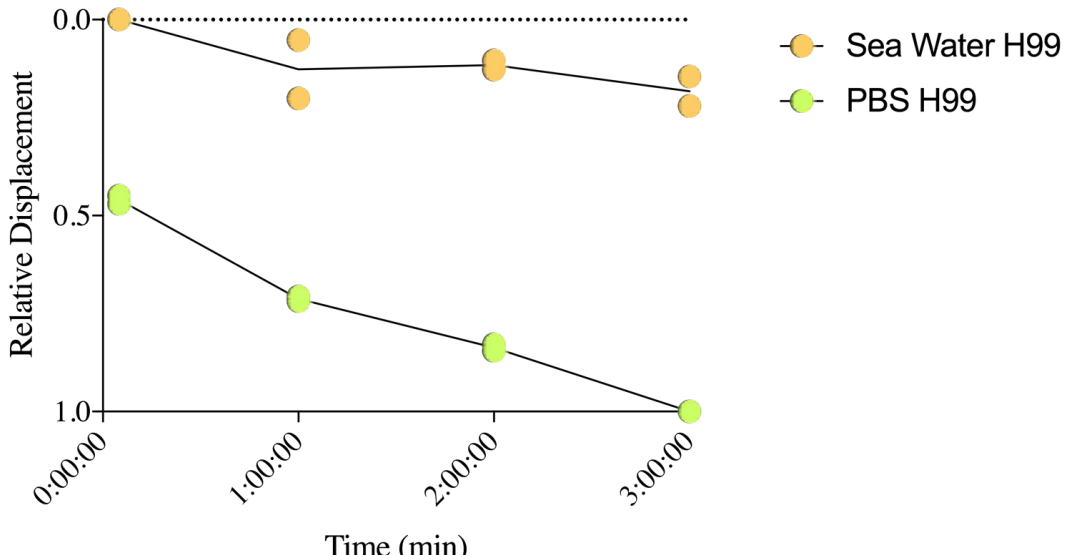
0.0
0.5
1.0
Relative Displacement
0:00:00
1:00:00
2:00:00
3:00:00
Time (min)
Sea Water H99
PBS H99